Lawrence Berkeley National Laboratory

Title
Radioisotope Yields from 1.85 GeV Protons on MO and 1.85- and5.0 GeV Protons on Te

Permalink
https://escholarship.org/uc/item/7cf6h3c4

Author
Bardayan, D.W.
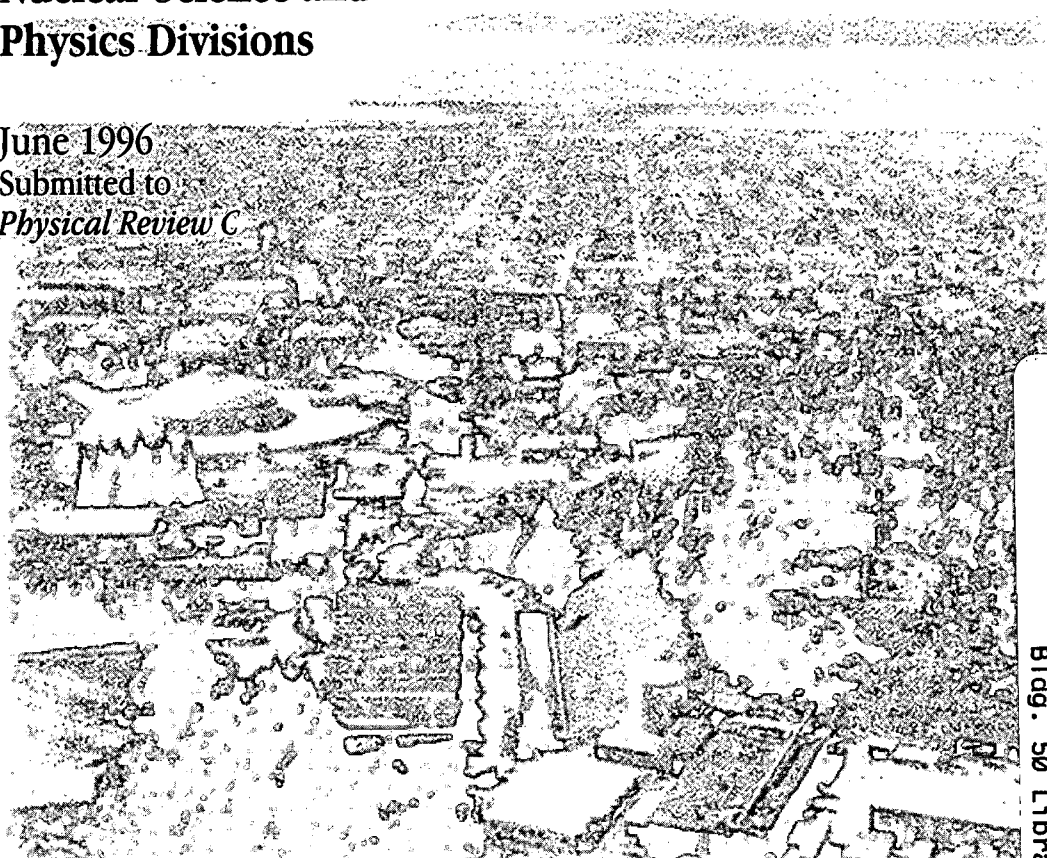
Publication Date
1996-06-06

ERNEST ORLANDO LAWRENCE BERKELEY NATIONAL LABORATORY

Radioisotope Yields from 1.85-GeV Protons on Mo and 1.85- and 5.0-GeV Protons on Te

D.W. Bardayan, M.T.F. da Cruz, M.M. Hindi,
A.F. Barghouty, Y.D. Chan, A. García,
R.-M. Larimer, K.T. Lesko, E.B. Norman,
D.F. Rossi, F.E. Wietfeldt, and I. Žlimen
**Institute for Nuclear
and Particle Astrophysics
Nuclear Science and
Physics Divisions**

DISCLAIMER

Radioisotope Yields from 1.85-GeV Protons on Mo and 1.85- and 5.0-GeV Protons on Te

D.W. Bardayan,[1] M.T.F. da Cruz,[2] M.M. Hindi,[1] A.F. Barghouty,[3] Y.D. Chan,[2]
A. García[2] R.-M. Larimer,[2] K.T. Lesko,[2] E.B. Norman,[2] D.F. Rossi,[2]
F.E. Wietfeldt,[2] and I. Žlimen[3]

[1]Physics Department, Tennessee Technological University, Cookeville, TN 38505
[2]Nuclear Science Division, Ernest Orlando Lawrence Berkeley National Laboratory,
University of California, Berkeley, CA 94270
[3]Physics Department, Roanoke College, Salem, VA 24153

June 1996

Radioisotope Yields from 1.85-GeV Protons on Mo
and 1.85- and 5.0-GeV Protons on Te

D. W. Bardayan,[1,*] M. T. F. da Cruz,[2,†] M.M. Hindi,[1] A. F. Barghouty,[3] Y. D. Chan,[2] A. García,[2,‡] R.-M. Larimer,[2] K. T. Lesko,[2] E. B. Norman,[2] D. F. Rossi,[2,§] F. E. Wietfeldt,[2,**] and I. Žlimen[3]

[1]*Physics Department, Tennessee Technological University, Cookeville, TN 38505, USA*

[2]*Nuclear Science Division, Lawrence Berkeley National Laboratory, Berkeley, CA 94720, USA*

[3]*Physics Department, Roanoke College, Salem, VA 24153, USA*

(June 6, 1996)

Abstract

Radioisotope yields from 1.85-GeV proton interactions in a natural isotopic composition Mo target and those from 1.85- and 5.0-GeV protons in natural Te targets were measured at Lawrence Berkeley National Laboratory's Bevatron. The radioisotope yields were determined by γ-counting the targets using 100-cm^3 coaxial Ge detectors following the irradiations. Cross sections were determined for the production of 36 radioactive nuclides, ranging from $Z = 35$,

---

*Present address: Physics Department , Yale University, New Haven, CT, USA.

†Present Address: Instituto de Física, Universidade de São Paulo, Caixa Postal 66318, 05389-970 São Paulo, SP, Brasil.

‡Present address: Physics Department, Notre Dame University, South Bend, IN, USA

§DOE-TRAC fellow at Lawrence Berkeley Laboratory, July-August 1992.

**Present address: National Institute of Science and Technology , Gaithersburg, MD, USA.

$A = 74$, to $Z = 43$, $A = 97$, from the Mo target and for 43 radioactive nuclides, ranging from $Z = 35$, $A = 75$, to $Z = 53$, $A = 130$ from the Te targets. The average deviations of the experimental cross sections from those predicted by the semi-empirical isotopic cross sections of Silberberg and Tsao were 53% for p+Mo at 1.85 GeV, 66% for p+Te at 1.85 GeV, and 35% for p+Te at 5.0 GeV. These deviations are higher than those found previously for medium and heavy targets and for elemental cross sections. The minimum production cross section of ^{91}Nb, which may be of interest as a cosmic-ray chronometer, was found to be 18 ± 3 mb for the p+Mo reaction.

PACS numbers: 25.40.Sc, 25.40.-h, 98.70.Sa

Typeset using REVTEX

I. INTRODUCTION

One of the keys to understanding the origin of galactic cosmic rays is a knowledge of the cosmic-ray composition at the source. This original composition is altered significantly by nuclear collisions with the interstellar medium as the cosmic rays propagate through it. Hence in order to infer the source composition from "local" measurements (here taken to mean in the vicinity of the solar system) calculations which model the propagation and interaction of cosmic rays in the interstellar medium are necessary. One of the essential ingredients in such calculations is the fragmentation cross section of abundant isotopes by collisions with the predominant interstellar medium – hydrogen. The projectile energy in these collisions spans a wide range, from a few hundred MeV/nucleon up to hundreds of TeV/nucleon. However, energies of the order of a few GeV/nucleon are the more dominant by virtue of the fact that the energy spectra of the arriving cosmic-ray flux seem to peak at around ~GeV/nucleon, for most of the observed cosmic-ray elements and after taking the solar modulation effects into account, and the fact that the spectra exhibit a strong power low ($\approx E^{-2.7}$) as a function of energy. Where available, experimental cross sections are used, otherwise semi-empirical equations are used. There is a clear need for the measurement of cross sections of the interaction of high energy protons on a wide range of nuclei, both for direct use in the propagation calculations and for further testing and fine tuning of the semi-empirical equations which are used to predict the unmeasured cross sections. Elemental production cross sections from interactions of relativisitic neon to nickel projectiles in hydrogen were recently reported by Knott et al. [1]. For reasons illucidated below, there is also a need for isotopic (versus elemental) cross sections for interactions with heavier nuclides. Here we report on isotopic production cross section from relativisitic proton interactions with molybdenum and tellurium targets.

Ultra-heavy (typically defined as those with $Z \geq 40$) cosmic-ray nuclides (UH-nuclides) have a special significance in both the nucleosynthesis as well as acceleration and propagation studies of cosmic rays. The nucleosynthesis of these UH-nuclides is due, for the most part,

3

to neutron capture reactions which start on the major product of charged-particle-induced nucleosynthesis, ^{56}Fe. In the slow (s-) process the neutron flux is so low that there is almost always sufficient time between neutron captures to allow β decay to occur. Thus the path of the s-process follows the line of β stability. In the r-process, by contrast, the neutron flux is so high that many neutron captures can occur before decay. Thus the r-process produces very neutron-rich nuclei which β decay back to stability once the neutron source turns off. Thus the r-process tends to produce the more neutron-rich stable isotopes.

The s-process produces approximately half of the nuclei between iron and bismuth. The s-process terminates at ^{209}Bi because addition of a neutron to this nucleus produces ^{210}Bi, which through alpha and beta decays eventually leads back to ^{206}Pb. The r-process produces most of the other half of the nuclei above iron and bypasses this bottle neck at ^{210}Bi. Thus the r-process alone is responsible for the production of uranium and thorium. It is generally believed that the site of the s-process is the helium burning zones of red-giant stars. The r-process is less understood, but it is thought that the conditions necessary to produce the high neutron fluxes required for the r-process can be achieved during supernova explosions. Thus, measurements of the cosmic-ray UH-nuclides and "propagating back" to the source (which requires knowledge of the relevant cross sections) should, in principle, delineate valuable information about the stellar environment and the nucleosynthesis therein.

There have been a number of recent (and/or planned) experiments to measure the cosmic-ray UH abundances: HEAO [2], ARIEL [3], TREK [4], TIGER [5], UHGCR [6], and HIIS [7]. The isotopic measurements presented here are well suited for comparisons to the widely-used Silberberg and Tsao (S&T) semi-empirical calculations [8] due to the sensitivity of the fragmentation cross sections to ΔA, the primary-secondary mass difference. The recent measurements of gold fragments at 10.6 GeV/nucleon (targets range from protons up to lead) of Waddington et al. [9] suggest that the S&T calculations tend to underestimate the small-ΔZ elemental yield by 20-30% when compared to the same reaction at 0.92 GeV/nucleon. This is compounded by the assertion that limiting fragmentation at that high energy is not yet reached, suggesting in turn some energy-dependence of the fragmentation cross sections.

The isotopic measurements presented here should help fine-tune both assertions, perhaps more quantitatively, due to the isotopic (rather than elemental) information offered, on the one hand, and due to our energies of 1.85 and 5 GeV, on the other. These energies happen to lie below the energy regime (around 10 GeV for proton-induced and around 2-3 GeV/ nucleon for heavy-ion-induced reactions [10,11]) where limiting fragmentation is suspected to have set in, yet slightly below and slightly above the assumed limit of around 3 GeV in the S&T semi-empirical calculations. In other words, the energy regime is such that, along with the isotopic information and when comparing to S&T predictions, more specific assertions about the correspondence of S&T predictions to measured fragmentation cross sections can be made. This, in turn, should help point to any need for improvement in the S&T predictions, for the UH-nuclides and at high energies, for more precise cosmic-ray propagation calculations.

In addition to the general aim of providing cross sections which would be useful for calibrating and extending the range of semi-empirical calculations into the heavy–UH element range, the experiment had the particular aim of measuring the yield of ^{91}Nb from the interaction of protons with molybdenum. In the laboratory, ^{91}Nb decays by electron capture (EC) with a 680 year half-life. However, as a high energy cosmic ray, it would be stripped of its atomic electrons and would be able to undergo only β^+ decay. ^{91}Nb can be produced in the cosmic rays through spallation of Mo and heavier elements by interstellar hydrogen [8]. Hence the cosmic ray half-life of ^{91}Nb depends on its β^+ partial half-life. This partial half-life has been recently measured to be $(8.8 \pm 1.9) \times 10^6$ years [12]. Since its half-life is on the order of millions of years, then ^{91}Nb could serve as another cosmic-ray chronometer and as a probe of models of the interstellar medium and of the propagation of this secondary component of cosmic rays. However, several problems must be overcome before ^{91}Nb can be used as a cosmic ray chronometer. In the cosmic rays there will be present three niobium isotopes: ^{91,92,93}Nb. ^{93}Nb is stable, is produced in stars via the s- and r-neutron capture processes, and will be injected into the cosmic rays. ^{91,92}Nb are expected to be present in the cosmic rays only as products of spallation reactions of molybdenum and heavier elements on interstellar

5

hydrogen. ^{92}Nb is an electron-capture-only nuclide which will become essentially stable as a bare cosmic ray nucleus, but ^{91}Nb will have a half-life of approximately 9 million years. Thus, in order to determine the age of these UH-nuclides, one will need to measure: 1) the isotopic composition of cosmic ray niobium, and 2) the relative ^{91}Nb and ^{92}Nb production cross sections from proton-induced spallation reactions on abundant heavier elements. With these purposes in mind, we set out to measure the production cross sections of these and other isotopes from the interaction of 1.85- and 5.0-GeV protons on Mo and Te targets.

II. EXPERIMENT

Targets of Mo and Te were bombarded with 1.85-GeV and 5.0-GeV protons from Lawrence Berkeley National Laboratory's Bevatron accelerator. For the 1.85-GeV irradiation the Mo and Te targets were each a disk of diameter 3.1 cm a thickness of 0.67 cm. For the 5.0-GeV irradiation the Te target was a block with an area of 5.1 cm ×5.1 cm and a thickness of 1.0 cm. The irradiation was performed with the targets in air, and with the Mo and Te slabs assembled in a stack, together with Polycast Acrylic sheets (polymethyl methacrylate, $[C_5O_2H_8]_n$). These plastic sheets served to monitor the integrated beam exposure, through the production of ^{11}C, from the C and O contents of the plastic [13,14]. The bombardment times were approximately 1 h each. Following each bombardment, the acrylic sheets were mounted at the center of a segmented annular NaI detector and the yield of ^{11}C was determined by measuring coincident 511-511 keV events. From these ^{11}C measurements we deduced integrated currents of 60 nC and 5 nC, respectively, for the 1.85-GeV and 5.0-GeV irradiations.

Following the irradiation, γ rays from each of the targets were counted (separately) with 100 cm^3 coaxial HPGe detectors inside a 5-cm thick lead shielding. Due to the widely different half-lives of the isotopes under study, three different lengths of time bins were used for counting: 5-min bins during the first two hours, 1-hour bins during the next 48 hours, and then a series of five 6-hours bins. Additionally, the Mo target was γ-counted again 49 days

6

later for a period of two days in order to specifically look for the decay of ^{91m}Nb ($t_{1/2} = 60.9$ days). An illustrative 1-h spectrum from the p+Mo irradiation is shown in Fig. 1.

III. DATA ANALYSIS AND RESULTS

The photo peak yields of characteristic γ rays of each isotope were extracted using a peak fitting routine. At least two γ-ray lines were used for each isotope, when possible. Tables 1 and 2 list the half-lives and characteristic γ rays that were used for each isotope, for Mo and Te, respectively. After correcting for the detector efficiency, self absorption in the target, summing and dead-time effects, the time-dependent yields of each γ-ray line were fit to determine initial activities. In some cases the time yields could be fit with two time components, thus allowing the extraction of the contribution of a parent nuclide to a daughter. Effective cross sections for the production of each isotope were calculated from a knowledge of the deduced yields at the end of the irradiation, the average proton flux and the duration of the irradiation.

Table 3 shows the measured effective cross-sections for radioisotopes produced in the p+Mo bombardment at 1.85 GeV, and Table 4 shows the cross sections for isotopes produced in the p+Te bombardment at 1.85 and 5.0 GeV. In those cases in which we determined the yield of a parent the direct production of the daughter isotope by spallation could be deduced. The cross section for such isotopes is marked as being direct in the Tables. Also listed in Tables 3 and 4 are the results of a theoretical calculation of the effective cross sections based on the semi-empirical formula given by Silberberg and Tsao [8]:

$$\sigma = \sigma_o f(A) f(E) \exp(-P\Delta A) \exp(-R|Z - SA + TA^2|^\nu)\Omega\eta\xi. \tag{1}$$

This equation is applicable for calculating cross sections of targets with $9 \leq A_T \leq 209$ and for products with $6 \leq A \leq 200$, except for peripheral interactions with very small ΔA. It is based on a semi-empirical spallation equation originally formulated by Rudstam [15], exploiting the systematic regularities in partial inelastic cross sections. In the above

7

Gaussian-like distribution (stemming from the statistical nature of nuclear evaporation), σ_o is a normalization factor, and the first exponential factor describes the diminution of σ as the target-product mass difference ΔA increases. The second exponential factor describes the distribution of cross sections for the production of various isotopes for a given atomic number Z. The width of the distribution is represented by the parameter R while S describes the location of the peak. The parameter T describes the shift of the distribution towards greater neutron excess as Z increases. The factors $f(A)$ and $f(E)$ apply to products from heavy targets with $Z_T > 30$. The parameter Ω is related to nuclear structure and number of particle-stable levels, while η depends on the pairing of protons and neutrons in a product nuclide, and ν is typically $\simeq 3/2$. The parameter ζ is introduced to reflect enhancements of light evaporation products. Typical values used for the factors and parameters appearing in Eq. (1) are tabulated in Ref. [8].

For the UH-nuclides reported in this work, an improved set of parameters was used that is applicable at high energies (for the 5 GeV measurements) and for $Z_T > 30$. [1] We mention here the more salient changes: The factor $Z - SA + TA^2$ in Eq. (1) is replaced with $Z - SA + TA^2 + UA^3$, with $U = 3 \times 10^{-7}$. Also, the functions $f(A)$ and $f(E)$ are $\neq 1$, which is the case for most other reactions. (The interested reader is referred to the Phys. Rep. part of Ref. [8] for the specific forms of $f(A)$ and $f(E)$ and for the numerical values of the parameters used.)

To give a general feeling for the degree of deviation between the measured yields and the S&T calculation we have plotted in Figs. 2–5 the ratio of the measured to calculated effective cross sections that were listed in Tables 3–4 as a function of the target-product mass difference ΔA (Figs. 2 and 4, for Mo and Te, respectively) and as a function of the target-product charge difference ΔZ (Figs. 3 and 5, for Mo and Te, respectively). The target masses were taken as the weighted averages over the isotopic abundances of Mo and Te (96.0

---

[1] See the Phys. Rep. part of Ref. 16, pp. 368).

8

for Mo and 127.7 for Te). For the data plotted as a function of ΔA, the cross sections at a given A (both the calculated ones and the measured ones) were summed over Z, while for the data plotted versus ΔZ the cross sections at a given Z were summed over A. For p+Mo at 1.85 GeV the median deviation between the measured isotopic cross sections and the S&T calculation is 40%, and the average is 53%. For p+Te at 1.85 GeV the median deviation is 45%, while the average deviation is 66%; the corresponding numbers for p+Te at 5.0 GeV are 44% (median) and 35% (average). These deviations are clearly larger than those for spallation reactions on medium and heavy targets (10–30%), and larger than those for the *elemental* production cross sections (20–30%).

The deviations plotted in Figs. 2–5 suggest that the S&T cross sections overestimate the yield for $\Delta A < 30$ and underestimate the yield for $\Delta A > 30$, with the discrepancy getting smaller at the higher (5 GeV) energy. For the Te data there seems to be an odd-even discrepancy for $\Delta A < 13$, the data showing larger variation between the yields of even and odd isotopes than is present in the calculations. Because the radioisotope yields measured here necessarily represent only a sampling of all the possible products of the reactions involved, we cannot assert that the above remarks are generally true.

The charge pickup reactions (resulting in the production of Tc and I from the Mo and Te targets, respectively) were excluded from Figs. 2–5 because of the possible substantial contribution of the interaction of low energy secondary protons to these cross sections. A rough estimate based on the measured yield of Iodine from the interaction of low energy (15–50 MeV) protons on Te [16] and assuming that on average one such low energy secondary proton is produced per primary interaction gives a contribution of about 1 mb to the production of ^{126}I. The possibility that this contribution is that high suggests that a more elaborate calculation, in which the yield and energy distribution of the secondary protons is properly taken into account, is required to estimate the contribution of secondary protons to the yield of Iodine (and Tc in the case of p+Mo). Since charge pickup reactions have relatively small cross sections, they have a minor effect on cosmic ray propagation calculations and we find no strong incentive at this stage to pursue an elaborate calculation (or to conduct thin target

9

measurements) to deduce these cross sections.

Apart from the charge pickup reactions mentioned above, the contributions of multiple interactions of the primary beam and of secondary spallation products to the measured yields are negligible. From the S&T total cross sections we estimate that the probability of interaction in the targets is about 3%; hence the multiple interactions of the beam contribute about 1.5% to the measured cross sections, a negligible amount for our purposes. The low energy neutrons produced by the spallation reactions will, at most, contribute to the yield of Mo and Te isotopes [via (n, xn) reactions] that are relatively close (in A) to the target isotopes; to the extent that the measured yields are less or comparable to the S&T yields, one concludes that the contribution of these secondary reactions must have been small.

Since the ^{91}Nb ground state, which has been proposed as a cosmic ray chronometer, has a half life of 680 y and no accompanying γ rays (save for the annihilation radiation from the weak β^+ branch [12]), it is extremely difficult to obtain its production cross section directly from our experiment. Our measurement of the production cross section of the ^{91}Nb^m isomer, which decays predominantly to the ground state, establishes a minimum production cross section of 18 ± 3 mb for the ground state. We have attempted to deduce the ^{91}Nb$^{g.s.}/^{91}$Nb^m relative production cross sections from the ground-state to isomer ratios observed for other isotopes in these measurements, but were unable to find a simple pattern to the observed ratios. In particular, the simple statistical ratio of $(2J_{g.s.}+1)/(2J_m+1)$ agreed well with some measured ratios but very poorly with others. The current S&T calculation does not give any predictions regarding the relative population of low lying states. Nevertheless, it is hoped that the minimum cross section reported here will help establish the feasibility of observing ^{91}Nb in cosmic rays, and that the measured cross sections for isotopes in the vicinity of ^{91}Nb, reported in this study, will help in improving the semi-empirical calculations to the point where they can reliably predict the ^{91}Nb, as well as other needed cross sections.

ACKNOWLEDGMENTS

REFERENCES

[1] Knott *et al.*, Phys. Rev. C **53**, 347 (1996).

[2] W. R. Binns, T. L. Garrard, P. S. Gibner, M. H. Israel, M. P. Kertzmann, J. Klarmann, B. J. Newport, E. C. Stone, and C. J. Waddington, Astrophys. J. **346**, 997 (1989).

[3] P. H. Fowler, R. N. F. Walker, M. R. W. Masheder, R. T. Moses, A. Morley, and A. M. Gray, Astrophys. J. **314**, 739 (1987).

[4] A. J. Westphal, P. B. Price, V. G. Afanasyev, V. V. Akimov, V. G. Rodin, G. K. Baryshnikov, L. A. Gorshkov, N. I. Shvets, and O. S. Tsigankov, Adv. Space Res. **15**, 605 (1995).

[5] W. R. Binns, *ibid*, 629 (1995).

[6] D. O'Sullivan, A. Thompson, K.-P. Wenzel, and F. Jansen, *ibid*, 625 (1995).

[7] J. H. Adams, Jr., L. P. Beahm, and A. J. Tylka, Proc. 22nd ICRC (Dublin), **2**, 523 (1991).

[8] R. Silberberg and C. H. Tsao, Astrophys. J. Supp. 25, 315 (1973); Phys. Rep. **191**, 351 (1990).

[9] C. J. Waddington, W. R. Binns, J. R. Cummings, T. L. Garrard, L. Y. Geer, J. Klarmann, and B. S. Nilson, Adv. Space Res. **15**, 639 (1995).

[10] L. Sihver *et al.*, Nucl. Phys. **A543**, 703 (1992).

[11] C. H. Tsao, R. Silberberg, A. F. Barghouty, and L. Sihver, Astrophys. J. **451**, 275 (1995); C. H. Tsao, R. Silberberg, A. F. Barghouty, L. Sihver, and T. Kanai, Phys. Rev. C **47**, 1257 (1993).

[12] M. M. Hindi, B. Sur, K. L. Wedding, D. W. Bardayan, K. R. Czerwinski, M. T. F. da Cruz, D. C. Hoffman, R.-M. Larimer, K. T. Lesko, E. B. Norman, Phys. Rev. C **47**, 2598 (1993).

[13] A. R. Smith, J. B. McCaslin, J. V. Geaga, J. C. Hill, and J. P. Vary, Phys. Rev. C **28**, 1684 (1983).

[14] D. L. Olson, B. L. Berman, D. E. Greiner, H. H. Hecjman, P. J. Lindstrom, and H. J. Crawford, Phys. Rev. C **28**, 1602 (1983).

[15] G. Rudstam, Z. Naturforsch A **21**, 1027 (1966).

[16] M. T. F. da Cruz, *et al.*, Phys. Rev. C **48**, 3106 (1993).

FIG. 1. One-hour γ-ray spectrum from Mo target after one hour of irradiation with 1.85-GeV protons.

FIG. 2. Ratio of the experimental to the Silberberg and Tsao effective cross sections for p+Mo at 1.85 GeV, plotted as a function of decrease in mass number. The initial A is taken as the weighted average for Mo (96.0). The cross section at a given A is the sum over Z of the cross sections listed in Table 3.

FIG. 3. Ratio of the experimental to the Silberberg and Tsao effective cross sections for p+Mo at 1.85 GeV, plotted as a function of decrease in atomic number. The cross section at a given Z is the sum over A of the cross sections listed in Table 3.

FIG. 4. Ratio of the experimental to the Silberberg and Tsao effective cross sections for p+Te at 1.85 GeV (solid circles joined by thick line) and 5 GeV (open squares joined by thin line), plotted as a function of decrease in mass number. The initial A is taken as the weighted average for Te (127.7). The cross section at a given A is the sum over Z of the cross sections listed in Table 4.

FIG. 5. Ratio of the experimental to the Silberberg and Tsao effective cross sections for p+Te at 1.85 GeV (solid circles joined by thick line) and 5 GeV (open squares joined by thin line), plotted as a function of decrease in atomic number. The cross section at a given Z is the sum over A of the cross sections listed in Table 4.

TABLES

TABLE I. Characteristic γ-ray lines and half-lives used in extracting cross sections for p+Mo at 1.85 GeV

Isotope	Half Life	E_γ(keV)
$^{74}Br^m$	42.0 min	635, 728
^{75}Br	1.6 h	287
^{76}Br	16.2 h	559, 657
^{77}Br	2.4 d	239, 521
^{76}Kr	14.8 h	316
^{77}Kr	1.2 h	130
^{79}Kr	1.5 d	398, 606
^{78}Rb	17.7 min	455
^{79}Rb	22.9 min	183, 688
^{81}Rb	4.6 h	190, 446
$^{82}Rb^m$	6.5 h	554, 619
$^{84}Rb^m$	20.3 min	216, 248
^{80}Sr	1.8 h	589
^{81}Sr	22.2 min	154
^{83}Sr	1.4 d	763
^{84}Y	40.0 min	793, 974
$^{85}Y^{g.s.}$	2.7 h	505
^{86}Y	14.7 h	1077, 1153
^{87}Y	3.3 d	388, 485
$^{90}Y^m$	3.2 h	202, 479
^{86}Zr	16.5 h	243
^{89}Zr	3.3 d	909
^{95}Zr	64.0 d	724, 757

^{97}Zr	16.9 h	658
^{88}Nb$^{g.s.}$	7.8 min	1057, 1083
^{88}Nb^{m}	14.3 min	1057, 1083
^{89}Nb^{m}	2.0 h	1628, 1834
^{90}Nb	14.6 h	1129, 2319
^{91}Nb^{m}	62.0 d	1205
^{92}Nb^{m}	10.2 d	935
^{95}Nb$^{g.s.}$	35.0 d	766
^{95}Nb^{m}	3.6 d	236
^{96}Nb	23.4 h	569, 1091
^{97}Nb	1.2 h	658
^{90}Mo	5.7 h	123, 258
^{93}Mo^{m}	6.9 h	685, 1477
^{93}Tc	2.8h	1363, 1520
^{95}Tc^{m}	61.0 d	204, 582

TABLE II. Characteristic γ-ray lines and half-lives used in extracting cross sections for p+Te at 1.85 and 5.0 GeV

Isotope	Half Life	E_γ(keV)
^{24}Na	14.7 h	1369
^{75}Br	1.6 h	287
^{76}Br	16.2 h	559, 657
^{77}Br	2.4 d	239, 521
^{82}Rb^m	6.5 h	554, 618, 776, 828, 1044, 1317
^{84}Rb^m	20.3 min	248
^{87}Sr^m	2.8 h	388
^{85}Y	2.7 h	505
^{86}Y	14.7 h	627, 1077, 1153, 1854, 1921
^{86}Y^m	48.0 min	208
^{87}Y	3.4 d	388, 485
^{87}Y^m	12.9 h	381
^{90}Y^m	3.2 h	479
^{86}Zr	16.5 h	243
^{87}Zr	1.7 h	381
^{90}Nb	14.6 h	132, 141, 1129, 2186, 2319
^{97}Ru	2.9 d	216, 324
^{100}Rh	20.8 h	540, 822, 1553, 2376
^{102}Rh^m	2.9 yr	475, 698, 631, 1047
^{107}In	32.0 min	205
^{108}In	40.0 min	633, 875
^{108}In^m	58.0 min	242, 633, 875
^{109}In	4.2 h	203

^{110}In	69.0 min	658
^{110}In^m	4.9 h	658, 707, 885, 937
^{111}In	2.8 d	171, 245
^{116}In^m	54.0 min	417, 1097, 1294
^{111}Cd^m	49.0 min	151, 245
^{116}Sb^m	1.0 h	407, 543, 844, 1072
^{117}Sb	2.8 h	159
^{118}Sb^m	5.0 h	254, 1051, 1230
^{120}Sb^m	5.8 d	90, 197, 1023, 1171
^{122}Sb	2.7 d	564, 693
^{125}Sb	2.7 yr	176, 601, 607, 636
^{126}Sb	12.4 d	297, 415, 666, 695, 697, 720, 856
^{126}Sb^m	19.0 min	415, 666, 695
^{127}Sb	3.8 d	253, 412, 474, 543, 686, 784
^{128}Sb	9.0 h	314, 526, 629, 636, 743, 754
^{128}Sb^m	10.4 min	314, 743, 754
^{129}Sb	4.4 h	181, 354, 544, 812, 914, 966, 1030
^{123}Sn	40.0 min	160
^{117}Te	61.0 min	720, 1716, 2300
^{119}Te	16.0 h	644
^{119}Te^m	4.7 d	154, 1213
^{121}Te	16.8 d	573
^{121}Te^m	154.0 d	212
^{129}Te	70.0 min	460, 487
^{121}I	2.1 h	212, 532
^{123}I	13.2 h	159

[124]I	4.2 d	603, 723, 1510
[126]I	13.0 d	389, 666
[128]I	25.0 min	443
[130]I	12.4 h	418, 536, 669, 739

TABLE III. Effective cross-sections for 1.85-GeV protons on natural Mo

| | cross section (mb) | |
Isotope	Expt.[a]	S&T[b]
$^{74}Br^m$	2.75(11)[c]	3.2
^{75}Br	8.7(3)	10.1
^{76}Br	10.1(9)[c]	12.0
^{77}Br	4.17(13)[c]	12.9
^{76}Kr	2.5(2)	4.3
^{77}Kr	4.58(15)	8.7
^{79}Kr	12.4(7)[c]	15.0
^{78}Rb	1.69(15)	2.5
^{79}Rb	5.1(6)	8.6
^{81}Rb	15.9(7)[c]	20.4
$^{82}Rb^m$	9.6(3)[c]	13.4
$^{84}Rb^m$	2.4(6)[c]	3.1
^{80}Sr	5.3(2)[c]	2.0
^{81}Sr	3.8(2)	4.7
^{83}Sr	18.6(6)	17.4
^{84}Y	7.2(2)	8.3
$^{85}Y^{g.s.}$	5.9(2)[c]	13.5
^{86}Y	15.8(6)[c]	13.1
^{87}Y	44.0(10)	30.1
$^{90}Y^m$	2.36(8)	4.2
^{86}Zr	8.1(2)	14.8
^{89}Zr	14.7(17)[c]	22.2
^{95}Zr	2.0(2)	3.3

20

^{97}Zr	2.10(5)	0.1
^{88}Nb$^{g.s.}$	2.7(2)	
^{88}Nb^m	5.2(8)	
^{88}Nb(tot)	7.9(8)	15.7
^{89}Nb^m	18.0(10)	22.8
^{90}Nb	26.2(8)^c	26.2
^{91}Nb^m	18.0(30)	35.7
^{92}Nb^m	13.6(5)^c	23.5
^{95}Nb$^{g.s.}$	18.5(9)^c	
^{95}Nb^m	5.0(4)^c	
^{95}Nb(tot)	23.5(10)^c	14.5
^{96}Nb	11.2(5)^c	10.3
^{97}Nb	9.9(5)^c	6.2
^{90}Mo	7.1(4)	7.1
^{93}Mo^m	2.8(1)^c	18.9
^{93}Tc	2.70(2)	0.3
^{95}Tc^m	2.0(5)^c	0.6

[a]Errors shown are statistical. There is an additional 10% error in the overall normalization of the cross-sections.

[b]Silberberg and Tsao cross section, reference [8].

[c]Direct production cross-section.

TABLE IV. Effective cross-sections (in mb) for 1.85- and 5.0-GeV protons on natural Te
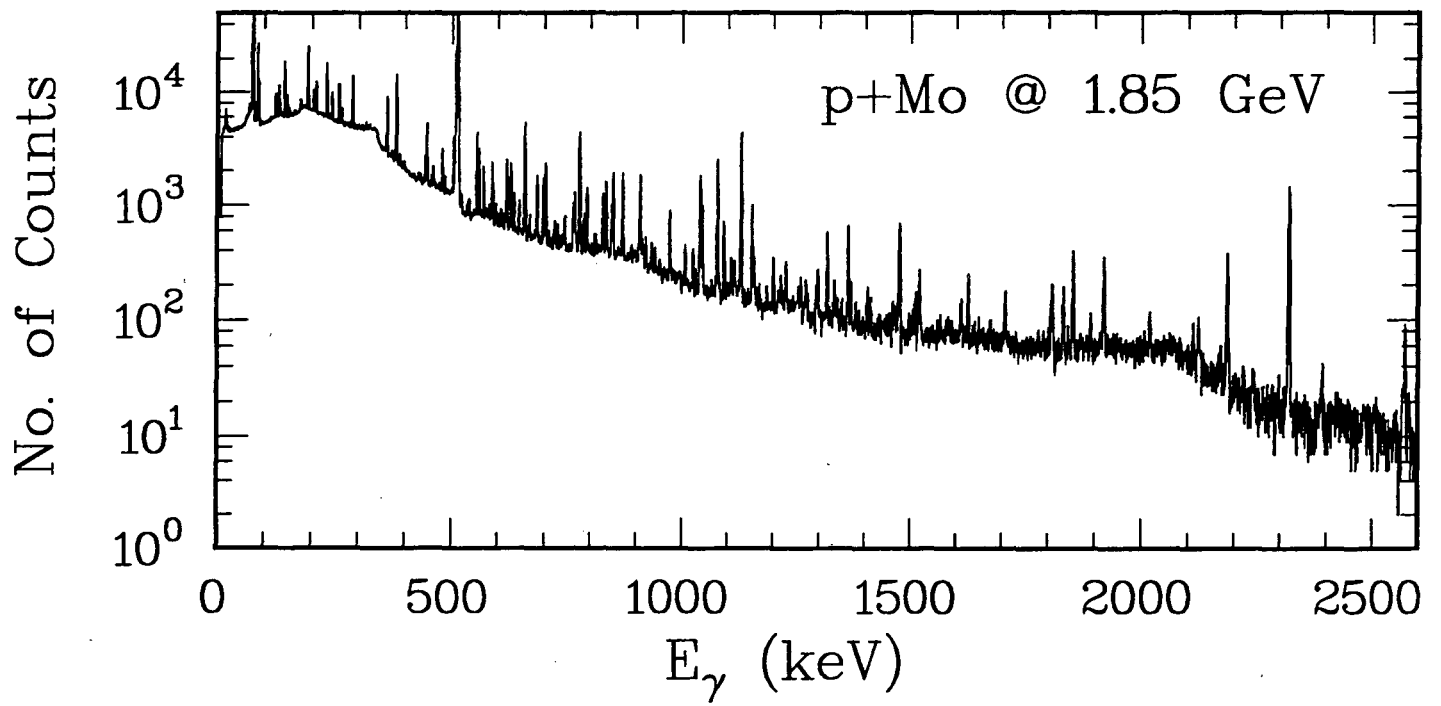
Isotope	1.85 GeV		5.0 GeV	
	Expt.[a]	S&T[b]	Expt.[a]	S&T[b]
^{24}Na	0.91(4)	0.73	4.4(2)	3.3
^{75}Br	1.30(3)	0.85	2.12(16)	2.43
^{76}Br	2.8(2)	1.8	3.7(3)	4.9
^{77}Br	4.6(2)	3.1	7.2(3)	8.2
^{82}Rb^m	3.3(1)[c]	2.6	4.1(2)[c]	5.9
^{84}Rb^m	1.4(3)[c]	0.8	2.3(2)[c]	1.6
^{85}Y	0.9(5)	2.6	-	5.6
^{86}Y$^{g.s.}$	19.0(10)[c]		23.0(10)[c]	
^{86}Y^m	5.2(1)[c]		6.1(1)[c]	
^{86}Y(tot)	24.2(10)[c]	3.5	29.1(10)[c]	7.2
^{87}Y^m	3.0(13)[c]		2.2(37)[c]	
^{87}Y$^{g.s.}$	0.55(33)[c]		-	
^{87}Y(tot)	3.6(13)[c]	3.9	2.2(37)[c]	7.7
^{90}Y^m	0.78(3)[c]	0.37	0.76(7)[c]	0.62
^{86}Zr	2.1(1)	0.32	2.8(1)	0.63
^{87}Zr	7.2(1)	1.0	10.0(20)	1.7
^{97}Ru	9.9(2)	6.4	9.7(3)	7.4
^{100}Rh	6.8(5)	8.2	6.2(2)	8.4
^{102}Rh^m	4.0(2)[c]	6.6	-	6.5
^{111}Cd^m	5.5(2)[c]	9.3	7.0(1)[c]	9.5
^{107}In	2.6(4)	2.7	2.0(2)	1.8
^{108}In$^{g.s.}$	1.2(1)			
^{108}In^m	3.2(1)[c]		2.7(2)[c]	
^{108}In(tot)	4.4(1)	6.4	>2.7(2)	3.9
^{109}In	9.1(1)	14.8	8.0(4)	9.5
^{110}In$^{g.s.}$	5.7(2)		4.4(1)	
^{110}In^m	4.1(2)		7.3(3)	
^{110}In(tot)	9.8(3)	18.8	11.7(3)	13.4
^{111}In	14.6(3)	24.4	16.4(4)	18.7
^{116}In^m	4.3(3)[c]	5.9	5.9(5)[c]	6.0
^{123}Sn	1.65(7)	7.4	2.93(15)	6.5
^{116}Sb^m	5.6(2)[c]	13.5	6.2(6)[c]	9.4
^{117}Sb	30.0(20)[c]	16.2	38.0(20)[c]	10.4
^{118}Sb^m	8.26(3)[c]	18.0	12.2(4)[c]	14.4
^{120}Sb^m	10.2(5)[c]	23.1	15.7(5)[c]	20.5
^{122}Sb	18.8(2)[c]	21.6	32.0(20)[c]	20.2

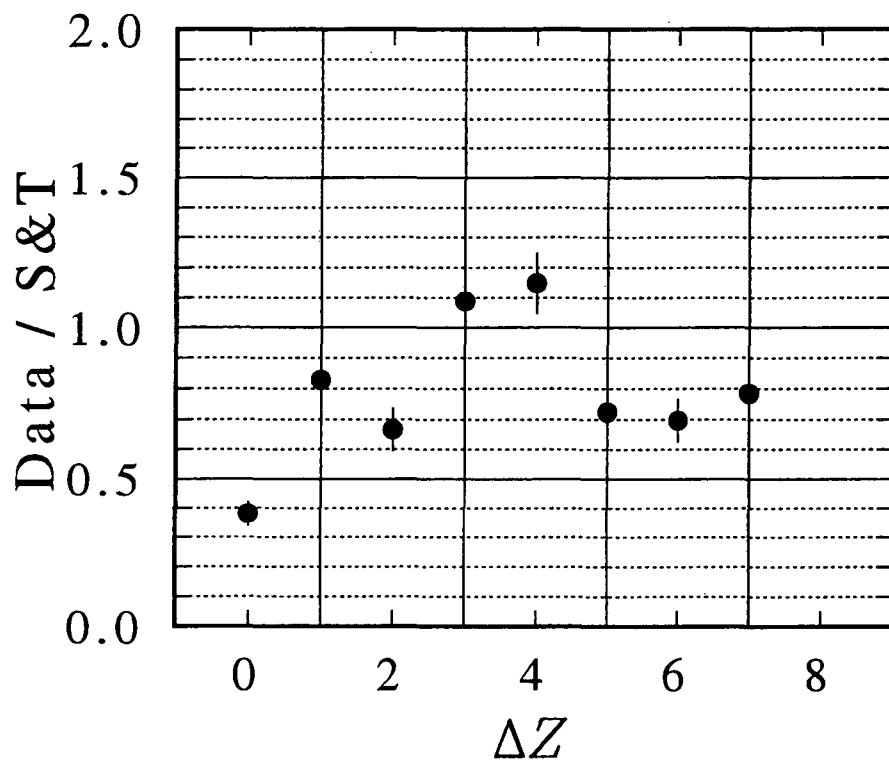|				
^{125}Sb	29.0(10)	18.8		
^{126}Sb$^{g.s.}$	4.8(4)[c]		7.9(3)[c]	
^{126}Sb^{m}	7.0(2)[c]		10.4(2)[c]	
^{126}Sb(tot)	11.8(2)[c]	13.5	18.3(4)[c]	13.5
^{127}Sb	11.8(4)	12.1	23.0(10)	12.1
^{128}Sb$^{g.s.}$	2.8(6)		3.7(2)	
^{128}Sb^{m}	3.1(2)		3.5(6)	
^{128}Sb(tot)	5.9(6)	6.6	7.2(6)	6.6
^{129}Sb	5.6(2)	4.4	8.8(8)	4.4
^{117}Te	4.6(3)	17.4	5.5(3)	7.0
^{119}Te$^{g.s.}$	4.31(15)		6.1(5)	
^{119}Te^{m}	9.2(7)		9.9(6)	
^{119}Te(tot)	13.5(7)	20.7	16.0(8)	9.9
^{121}Te$^{g.s.}$	8.3(4)[c]		9.5(4)[c]	
^{121}Te^{m}	14.0(40)[c]		22.0(20)[c]	
^{121}Te(tot)	22.3(40)[c]	16.7	31.5(20)[c]	12.4
^{129}Te	25.0(10)[c]	24.6	52.0(30)[c]	24.6
^{121}I	3.7(1)[c]	1.0	6.2(2)[c]	0.6
^{123}I	9.0(2)[c]	1.4	11.7(3)[c]	1.0
^{124}I	9.4(3)[c]	1.5	15.2(5)[c]	1.2
^{126}I	6.9(23)[c]	1.2	15.0(60)[c]	1.2
^{128}I	5.7(4)[c]	0.8	10.0(20)[c]	0.8
^{130}I	3.0(1)[c]	0.3	4.6(9)[c]	0.3

[a]Errors shown are statistical. There is an additional 10% error in the overall normalization of the cross-sections.
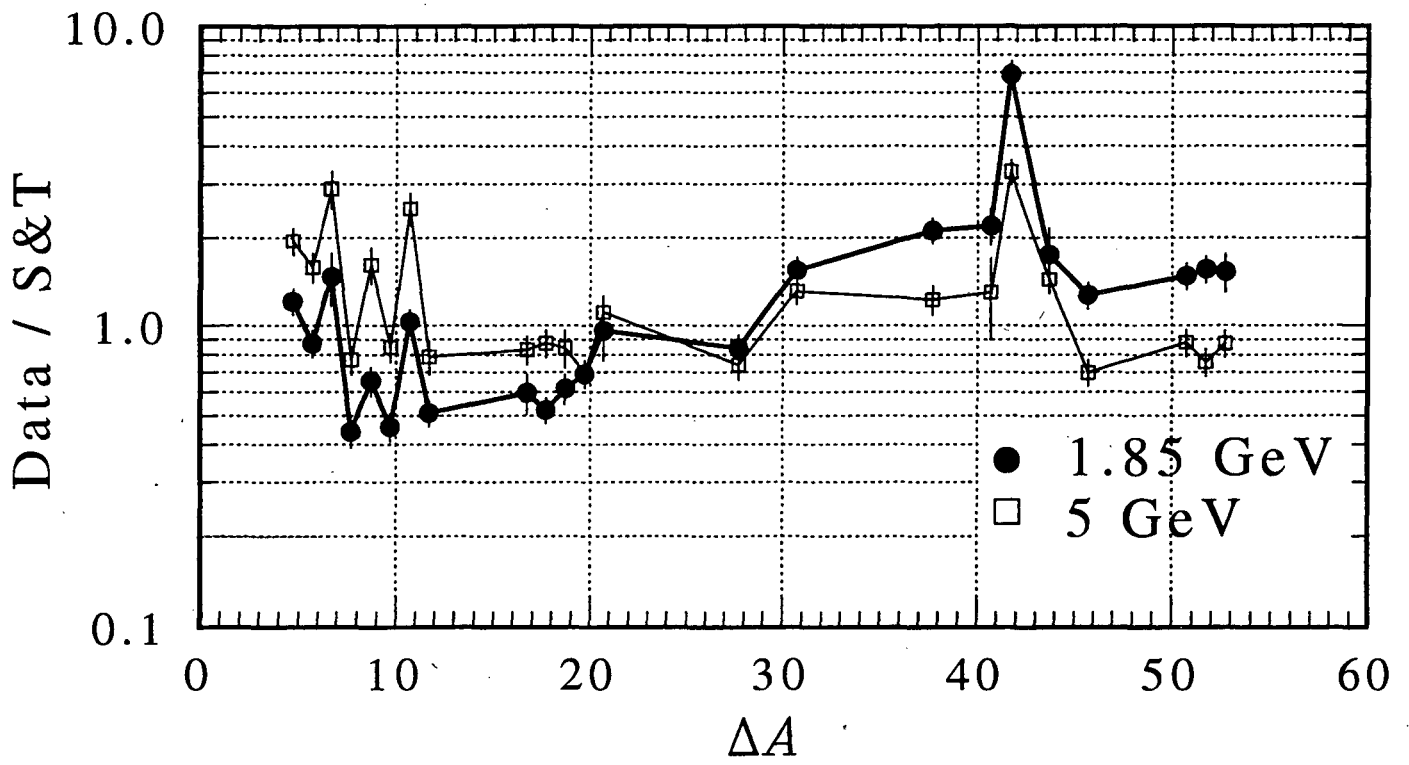
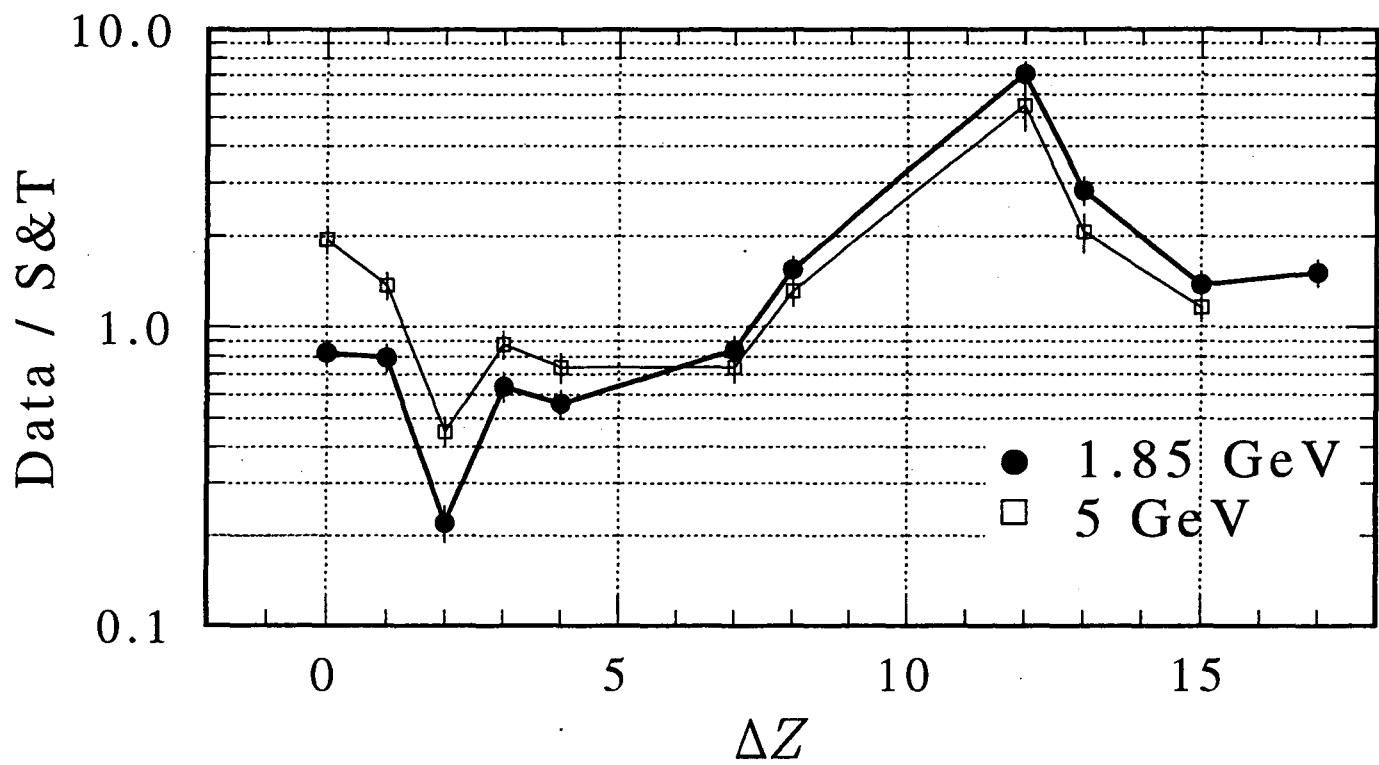[b]Silberberg and Tsao cross section, reference [8].

[c]Direct production cross-section.

p+Mo @ 1.85 GeV